

Synthesis, crystal structures and phosphodiesterase activities of alkoxide-bridged asymmetric dinuclear nickel(II) complexes

Ai-zhi Wu · Tao Wang

Received: 17 October 2013 / Accepted: 2 December 2013 / Published online: 13 December 2013
© Springer Science+Business Media Dordrecht 2013

Abstract An asymmetric dinuclear ligand, *N*-4-methyl-homopiperazine-*N'*-[*N*-(2-pyridylmethyl)-*N*-2-(2-pyridylethyl)amine]-1,3-diaminopropan-2-ol (HL) and two dinuclear Ni(II) complexes [Ni₂L(DNBA)₂]ClO₄ (**1**) and [Ni₂L(BPP)₂]ClO₄·2H₂O (**2**) (3,5-dinitrobenzoic acid, bisphenyl phosphate) have been synthesized and characterized. Single crystal X-ray crystallographic analysis reveals that the coordination environments of the two Ni(II) atoms in complexes **1** and **2** are five and six coordinate, respectively. The phosphodiesterase activity of a di-Ni(II) complex Ni₂L formed in situ from a 2:1 mixture of Ni²⁺ and HL was investigated using bis(4-nitrophenyl) phosphate (BNPP) as the substrate. The pH dependence of the rate of BNPP cleavage in aqueous buffer indicates a bell-shaped profile with an optimum at about pH 8.4, which is parallel to the formation of the dinuclear species [Ni₂LOH]²⁺ according to UV–vis spectroscopy. At pH 8.4 and 25 °C, the *k*_{cat} (7.40 × 10⁻⁵ s⁻¹) is ca.10⁶-fold higher than that of the uncatalyzed reaction. A possible mechanism for BNPP cleavage promoted by Ni₂L is proposed.

Introduction

Kidney bean purple acid phosphatases belonging to the family of binuclear metallohydrolases and are involved in a multitude of biological functions. These enzymes require structurally asymmetric Fe(III) and Zn(II) or Fe(II) centers in the active sites, reflecting the different roles played by

the two metal ions [1–3]. Although different coordination environments are found for the metal centers in this dinuclear metalloenzyme, a large number of the enzyme mimics reported so far are based on symmetric dinucleating ligands with identical coordination geometries for the two metal centers [4–13]. Less attention has been paid to the preparation of asymmetric dinuclear complexes, especially dinickel(II) complexes [14–18]. The synthesis and comparison of asymmetric and symmetric dinuclear enzyme models should provide a deeper insight into the structure and mechanism of the natural enzymes, and so help to design more effective metalloenzyme models. Herein, we describe the synthesis and characterization of a new asymmetric dinuclear ligand, *N*-4-methyl-homopiperazine-*N'*-[*N*-(2-pyridylmethyl)-*N*-2-(2-pyridylethyl)amine]-1,3-diaminopropan-2-ol (HL), and its dinuclear Ni(II) complexes [Ni₂L(DNBA)₂]ClO₄ (**1**) and [Ni₂L(BPP)₂]ClO₄·2H₂O (**2**) which are exogenously bridged by carboxylate and phosphate ester ligands, respectively. Further, the phosphodiesterase activity of the dinuclear Ni(II) complex formed in situ from HL and nickel(II) in aqueous solution was investigated using bis(4-nitrophenyl) phosphate (BNPP) as a model substrate.

Experimental

Materials and methods

¹H NMR spectra were measured on a Bruker AM-400 spectrometer. FTIR spectra were recorded on an Equinox 55 spectrophotometer using KBr pellets (4,000–400 cm⁻¹). Mass spectra were measured on a Thermo Finnigan TSQ mass spectrometer. Elemental analyses were obtained on a Vario EL-III instrument. The pH measurements were

A. Wu (✉) · T. Wang
School of Chinese Materia Medica, Guangzhou University of Chinese Medicine, Guangzhou 510006,
People's Republic of China
e-mail: wuaizhi@gzucm.edu.cn

carried out with an Orion 420A pH meter with an Aldrich combination pH electrode, calibrated with standard buffers (pH = 4.01, 7.00 and 10.01, Sigma). Kinetic measurements were recorded using quartz cuvettes (1 cm) with Teflon stoppers on a U-3100 UV–vis spectrophotometer. The buffer solutions were prepared with HEPES (*N*-[2-Hydroxyethyl]piperazine-*N'*-[2-ethanesulfonate]) and CHES ((2-cyclohexylamino)ethanesulfonate) and adjusted to the desired pH by adding freshly prepared NaOH solution. HBNPP purchased from Aldrich was recrystallized from ethanol/water before use. NaBPP was synthesized by mixing NaOH and bisphenyl phosphate (HBPP) in 1:1 ratio in aqueous solution, and the pure product was obtained as a white powder after the evaporation of water. Elemental analysis was performed to confirm the composition and purity of NaBPP. *N*-(2-Pyridyl)methyl-*N*-2-(2-pyridylethyl)amine (**I**) was prepared as described in the literature [17].

Synthesis of *N*-(2-pyridylmethyl)-*N*-2-(2-pyridylethyl) [(3-chloro)(2-hydroxy)] propylamine (**II**)

A solution of **I** (2.09 g, 9.8 mmol) in methanol (15 mL) was added to a stirred solution of epichlorohydrin (0.93 g, 10 mmol) in methanol (15 mL) at 0 °C. After addition, the reaction mixture was stirred for 72 h at room temperature, resulting in a reddish solution. The solvent was removed under reduced pressure at 35 °C, and the residue was dissolved in dichloromethane (50 mL). The solution was extracted with successive portions of brine (25 mL each) until the aqueous phase became colorless. The organic layer was dried over anhydrous Na₂SO₄ and filtered; the solvent was removed under reduced pressure at 30 °C, resulting in a light orange oil with 78 % yield. ¹HNMR (CDCl₃): δ = 8.52, 2H; 7.4–7.6, 2H; 7.2–6.8, 4H; 7.08, 2H; 3.95–3.9, 3H; 3.53, 2H; 2.80–3.00, 7H. FTIR (KBr, cm⁻¹): 3351(w, s), 2954 (s), 2830(s), 1594(s), 1570(s), 1475(s), 1437(s), 1366(s), 1305(s), 1256(s), 1122(s), 1094(s), 1052(s), 1001(s), 894(s), 761(s), 622(s).

Synthesis of *N*-4-methyl-homopiperazine-*N'*-[*N*-(2-pyridylmethyl)-*N*-2-(2-pyridylethyl) amine]-1, 3-diaminopropan-2-ol (HL)

A mixture of 1-methyl-homopiperazine (1.14 g, 10 mmol) and triethylamine (4.16 mL, 30 mmol) in acetonitrile (20 mL) was added to a stirred solution of **II** (3.05 g, 10 mmol) in dry acetonitrile (40 mL) at 0 °C. After the addition, the reaction mixture was stirred for 48 h at room temperature and then for 72 h at 40 °C. After cooling to 0 °C, the resulting white precipitate was filtered off. Evaporation of the solvent under reduced pressure produced a brown oil, which was dissolved in water (30 mL)

and extracted with dichloromethane. The organic phase was dried over Na₂SO₄. Evaporation of the solvent yielded an orange oil which was further purified by silica gel chromatography using chloroform/methanol (10/1, v/v) as eluent. The pure ligand HL was obtained as a light orange oil with 36 % yield. ¹HNMR (CDCl₃): δ = 8.52, 2H; 7.58, 2H; 7.2–7.08, 4H; 4.0–3.85, 3H, 3.05–2.95, 4H, 2.90–2.38, 16H, 1.82–1.78, 2H. FTIR (KBr, cm⁻¹): 3381(w, s), 2939(s), 2811(s), 1661(s), 1594(s), 1475(s), 1435(s), 1366(s), 1309(s), 1126(s), 1051(s), 1001(s), 763(s), 624(s).

Synthesis of [Ni₂L(DNBA)₂]ClO₄ (**1**)

A solution of Ni(ClO₄)₂·6H₂O (53 mg, 0.146 mmol) in methanol (1 mL) was added to a stirred solution of HL (28 mg, 0.073 mmol) in methanol (1 mL). Next, a solution of Et₃N (10 μL, 0.073 mmol) in methanol (1 mL) was added where upon a red solution was formed. This was stirred at room temperature for 1 h, and then, a solution of DNBA (31 mg, 0.146 mmol) and Et₃N (20 μL, 0.146 mmol) in methanol (1 mL) was added. The color of the solution rapidly changed from red to green, and then, a green precipitate was formed slowly. The mixture was stirred at room temperature for another 1 h, and then, the crude product was collected by filtration and washed with methanol. Green block crystals were obtained by recrystallization from 2:1 MeCN-EtOH solution (3 mL) with a yield of 65 %. Anal. Calcd for C₃₆H₃₈ClN₉O₁₇Ni₂. Found (calcd): C, 38.6 (38.4); H, 3.5 (3.7); N, 12.1 (12.3). FTIR (KBr, cm⁻¹): 3434(w), 3106(s), 2911(s), 2862(s), 1633(s), 1574(s), 1539(s), 1480(s), 1457(s), 1400, (s) 1349(s), 1268(s), 1202(s), 1088(w) (s), 920(s), 869(s), 788(s), 763(s), 724(s), 675(s), 645(s), 622(s), 527(s), 486(s).

Synthesis of [Ni₂L(BPP)₂]ClO₄·2H₂O (**2**)

A solution of Ni(ClO₄)₂·6H₂O (73 mg, 0.2 mmol) in water (1 mL) was added to a stirred solution of HL (28 mg, 0.073 mmol) and Et₃N (10 μL, 0.073 mmol) in water (2 mL). Next, a solution of NaBPP (55 mg, 0.2 mmol) in water (1 mL) was added. The color of the solution rapidly changed from red to green, and then, a green precipitate was formed slowly. The mixture was stirred at room temperature for 1 h, after which the crude product was collected by filtration and washed with water and ethanol. Green block crystals were obtained by recrystallization from 2:1 CH₃CN-EtOH solution (3 mL) with a yield of 70 %. Anal. Calcd for C₄₆H₅₆ClN₅O₁₄P₂Ni₂. Found (calcd): C, 48.7 (49.4); H, 3.8 (5.0); N, 6.5 (6.3). IR (KBr, cm⁻¹): 3445(w), 3066(s), 2859(s), 1593(s), 1489(s), 1443(s), 1320(s), 1259(s), 1205(s), 1162(s), 1092(s), 1023(s), 918(s), 777(s), 764(s), 692(s), 526(s).

Table 1 Crystal data and structure refinement for complexes **1** and **2**

Complexes	1	2
Empirical formula	C ₃₆ H ₃₈ ClN ₉ Ni ₂ O ₁₇	C ₄₆ H ₅₆ ClN ₅ Ni ₂ O ₁₄ P ₂
Formula weight	1021.62	1117.77
Crystal size (mm)	0.18 × 0.08 × 0.03	0.30 × 0.20 × 0.02
T (K)	298(2) K	173(2) K
Wavelength	0.71073 Å	0.71073 Å
Crystal system	Monoclinic	Monoclinic
Space group	P2(1)/c	P2(1)/c
<i>a</i> (Å)	15.8271(10)	14.5728(9)
<i>b</i> (Å)	18.7181(8)	19.1305(9)
<i>c</i> (Å)	15.4805(10)	20.0043(12)
α (°)	90°	90°
β (°)	113.527(7)°	90.710(5)°
γ (°)	90°	90°
<i>V</i> (Å ³)	4204.9(4)	5576.5(5)
<i>Z</i>	4	4
Density (g cm ⁻³)	1.614	1.331
<i>F</i> (000)	2104	2328
Absorption coefficient (mm ⁻¹)	2.449	2.354
Data/restraints/parameters	7757/0/582	8016/0/622
θ range for data collection (°)	3.85–72.34	3.03–67.00
Reflections collected	19243	14676
Independent reflections	7757 (<i>R</i> _{int} = 0.0887)	8016 (<i>R</i> _{int} = 0.0495)
GOF on <i>F</i> ²	0.843	1.148
Final <i>R</i> indices [<i>I</i> > 2σ(<i>I</i>)] ^a	<i>R</i> ₁ = 0.0584, <i>wR</i> ₂ = 0.0956	<i>R</i> ₁ = 0.1151, <i>wR</i> ₂ = 0.3181
<i>R</i> indices (all data) ^a	<i>R</i> ₁ = 0.1475, <i>wR</i> ₂ = 0.1205	<i>R</i> ₁ = 0.1654, <i>wR</i> ₂ = 0.3510
Largest different peak and hole (e.Å ⁻³)	0.366 and -0.310	1.349 and -0.558

Single crystal X-ray crystallography

The green crystals of **1** and **2** were mounted on glass fibers and used for data collection. Single X-ray diffraction data were obtained on a Bruker Smart Apex CCD area detector using graphite monochromated Mo K α radiation ($\lambda = 0.71073$ Å). The structure was solved by direct methods and refined on *F*² by full-matrix least squares techniques with SHELXTL-97 [19]. All non-hydrogen atoms were refined anisotropically, and all hydrogen atoms of the ligands were located and included at their calculated positions. Crystallographic data for complexes **1** and **2** have been deposited at the Cambridge Crystallographic Data Center, CCDC No. 966148 for **1**, and 966149 for **2**, respectively. The crystal data and structure refinement are summarized in Table 1, and selected bond lengths and bond angles are listed in Table 2.

Cleavage of BNPP

The cleavage of BNPP was monitored in a buffered aqueous solution (*I* = 0.1 M NaClO₄, *T* = 25 °C) by

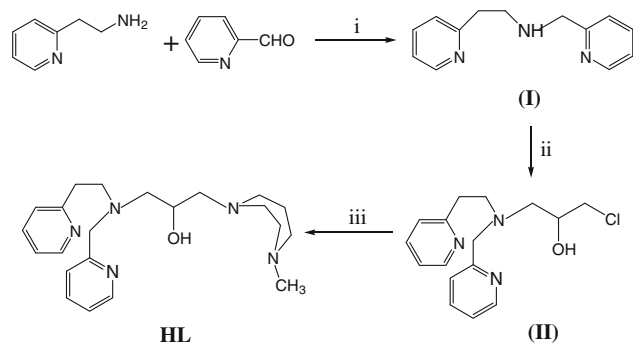
detecting the increase in the maximum absorbance at 400 nm of the 4-nitrophenolate anion (NPat), using an extinction coefficient of 18,700 L mol⁻¹ [20]. In a typical experiment, a solution of Ni₂L was prepared by thoroughly mixing 40 μ L of stock solution of HL (50 mM in water) and Ni(ClO₄)₂ (100 mM in water) in containing 1.92 mL of 0.05 M buffer solution for 30 min at 25 °C. An aliquot of 50 μ L of BNPP solution (40 mM in water) was then added to the solution of the complex in a cuvette and mixed well. The final concentrations of Ni₂L and BNPP were both 1 mM. After addition, the mixture was allowed to equilibrate for 5 min and the reactions were followed up to 5 % BNPP cleavage. The absorbance values were converted into the concentration of the NPat ion, and the total analytic 4-nitrophenol product was calculated using the buffer pH and the *p*K_a of 4-nitrophenol (7.15) [21].

Results and discussion

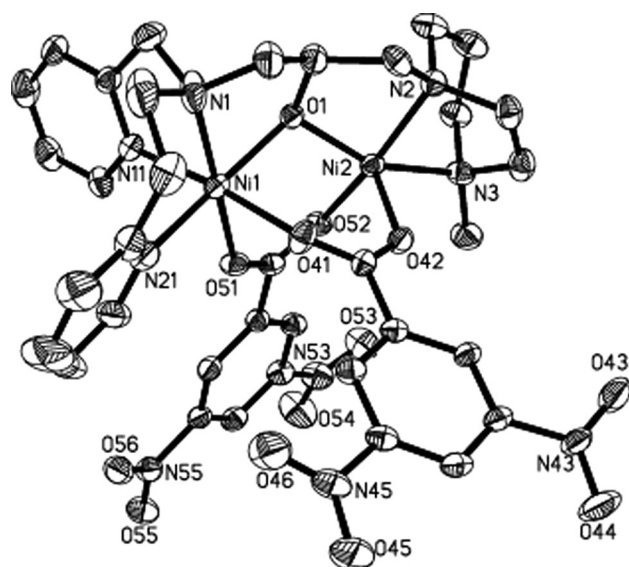
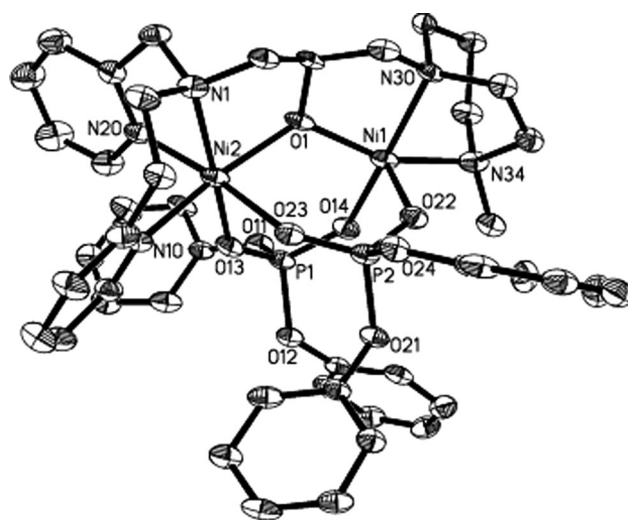
The synthetic route to the asymmetric ligand HL is illustrated in Scheme 1. The introduction of the asymmetry, the

Table 2 Selected bond lengths (Å) and angles (°) for complexes **1** and **2**

1		2	
<i>Bond lengths</i>			
Ni(1)–O(1)	2.023(3)	Ni(1)–O(1)	1.953(8)
Ni(1)–O(41)	2.127(3)	Ni(1)–O(14)	1.975(7)
Ni(1)–O(51)	2.070(3)	Ni(1)–O(22)	1.992(7)
Ni(1)–N(1)	2.109(5)	Ni(1)–N(30)	2.037(7)
Ni(1)–N(11)	2.082(4)	Ni(1)–N(34)	2.064(10)
Ni(1)–N(21)	2.099(5)	Ni(2)–O(1)	2.057(6)
Ni(2)–O(1)	1.957(3)	Ni(2)–O(13)	2.086(7)
Ni(2)–O(42)	1.986(3)	Ni(2)–O(23)	2.188(8)
Ni(2)–O(52)	1.991(3)	Ni(2)–N(1)	2.101(8)
Ni(2)–N(2)	2.051(4)	Ni(2)–N(10)	2.098(8)
Ni(2)–N(3)	2.056(4)	Ni(2)–N(20)	2.102(10)
Ni(1)⋯Ni(2)	3.305	Ni(1)⋯Ni(2)	3.558
<i>Bond angles</i>			
O(1)–Ni(1)–N(21)	166.98(16)	O(1)–Ni(1)–N(30)	86.1(3)
O(1)–Ni(1)–O(41)	87.78(13)	O(1)–Ni(1)–O(14)	98.3(3)
N(1)–Ni(1)–N(11)	82.9(2)	N(30)–Ni(1)–N(34)	77.6(4)
O(1)–Ni(1)–N(1)	78.96(18)	O(1)–Ni(1)–O(22)	100.0(3)
N(1)–Ni(1)–O(41)	98.80(19)	N(1)–Ni(2)–N(20)	80.0(3)
O(1)–Ni(2)–O(52)	97.47(13)	O(1)–Ni(2)–N(10)	165.8(3)
O(1)–Ni(2)–O(42)	103.13(14)	O(1)–Ni(2)–O(23)	84.0(3)
N(2)–Ni(2)–O(52)	163.05(15)	O(23)–Ni(2)–O(13)	91.7(3)
O(1)–Ni(2)–N(3)	156.35(16)	O(1)–Ni(2)–N(20)	103.1(3)
N(2)–Ni(2)–N(3)	78.29(17)	N(10)–Ni(2)–N(20)	89.7(3)
Ni(1)–O(1)–Ni(2)	112.27(15)	Ni(1)–O(1)–Ni(2)	125.1(3)

**Scheme 1** Synthetic route to the ligand HL^a

key step in the synthesis, is realized through opening of the epoxyethane ring in the epichlorohydrin, which also offers a chloromethyl group for the alkylation of a second amine different from the first. The overall synthesis involves three reactions and affords the desired ligand in gram quantities with an overall yield of ca. 32 %.

**Fig. 1** ORTEP drawing of the cationic structure in **1**. Thermal ellipsoids for the non-hydrogen atoms are drawn at the 30 % probability level. All hydrogen atoms are omitted for clarity**Fig. 2** ORTEP drawing of the cationic structure in **2**. Thermal ellipsoids for the non-hydrogen atoms are drawn at the 30 % probability level. All hydrogen atoms are omitted for clarity

Crystal structure analysis of complexes **1** and **2** shows that they both crystallize in a monoclinic P2(1)/c space group with a mono-cation of $[\text{Ni}_2\text{L}(\text{DNBA})_2]^+$ and $[\text{Ni}_2\text{L}(\text{BPP})_2]^+$, respectively, and one ClO_4^- acting as the counter anion. Ellipsoid drawings of the cationic cores in **1** and **2** are depicted in Figs. 1 and 2, respectively. In complex **1**, the two nickel atoms are bridged by the ionized alkoxide oxygen of L and two carboxyl groups from the DNBA ligand in μ -bridging mode. In the bipyridyl pendant, the six-coordinated environment around Ni(1) is comprised of the N_3O donor set from L and two oxygen

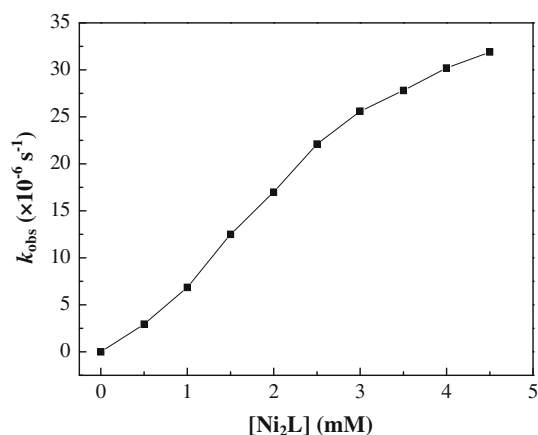


Fig. 3 Dependence of k_{obs} on the concentration of $[\text{Ni}_2\text{L}]$ in buffer solution (50 mM HEPPS and 100 mM NaClO_4 in water, pH = 8.4) at 25 °C, $[\text{BNPP}] = 1 \text{ mM}$

atoms from the bridging carboxyl groups, while in the homopiperazine pendant, the N_2O donor set from L, plus two bridging oxygen atoms, provides the distorted square-pyramidal geometry around Ni(2), with the atom O(42) occupying the apical position in the coordination sphere. Complex **2** is almost isostructural with **1**, except that the two exogenous carboxyl bridges are replaced by two phosphate groups of BPP. The bond lengths of Ni(1)–O(1) and Ni(2)–O(1) in complex **2** are similar to those observed in **1**. However, the Ni–O–Ni angle and Ni⋯Ni distance are slightly larger than those observed in **1**, which is partly caused by the bulky size of the BPP bridges in **2**. To bind the nickel atom in a chelating mode, the seven-membered homopiperazine ring has to adopt a less stable boat-shape conformation, and the corresponding bond angles N(2)–Ni(2)–N(3) in **1** and N(30)–Ni(1)–N(34) in **2** are 78.3(2)° and 77.6(4)°, respectively. These values deviate significantly from the normal bond angle observed in complexes with square-pyramidal geometry, suggesting that the homopiperazine pendant is in a strained geometry.

Phosphodiesterase activity of Ni_2L

Bis(4-nitrophenyl) phosphate is often used as a DNA model compound in the investigation of phosphodiesterase activity. The tests for phosphodiesterase activity were carried out in buffers in order to mimic biological conditions. The reaction was monitored by following the release of NP from BNPP. The dependence of the reaction rate on pH for the BNPP cleavage promoted by dinuclear species Ni_2L formed in situ from a 2:1 mixture of Ni^{2+} and ligand HL in aqueous solution shows a bell-shaped profile, with an optimum at about pH 8.4. The ES-MS spectrum of Ni_2L in aqueous solution displayed a peak at $m/z = 615$, corresponding to the $[\text{Ni}_2\text{L}(\text{OH})(\text{ClO}_4)]^+$ ion. Moreover, at pH

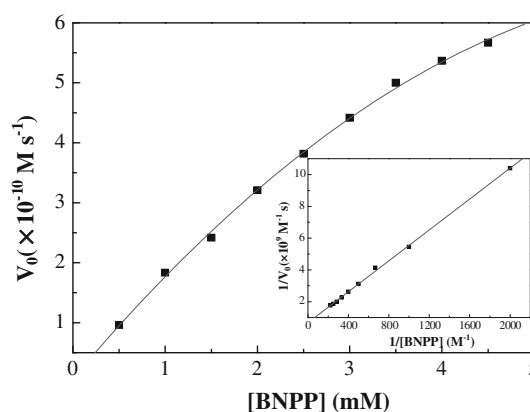
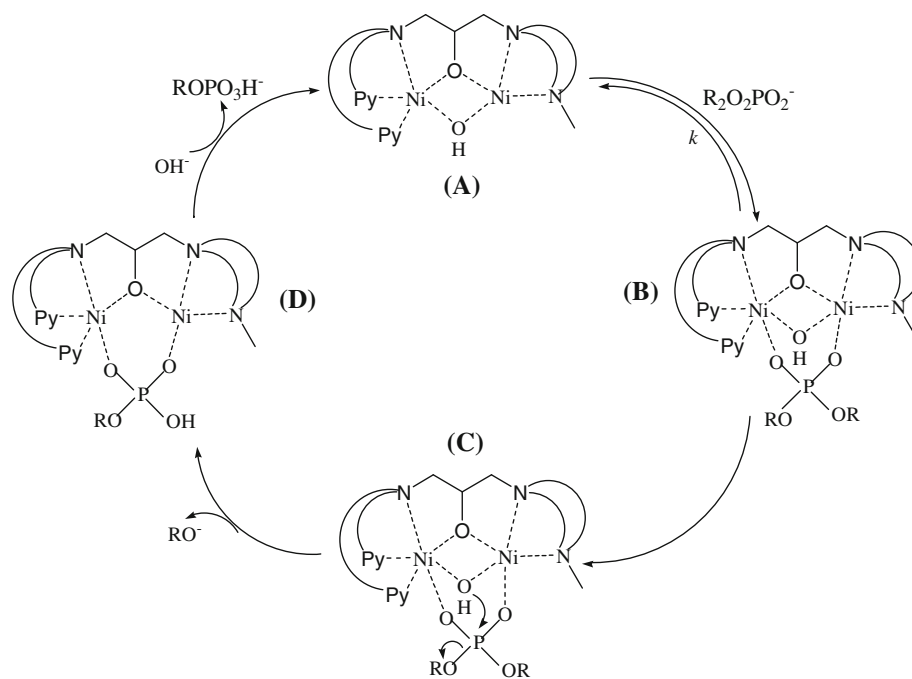


Fig. 4 Saturation kinetic experiments for the cleavage of BNPP by $[\text{Ni}_2\text{L}]$ at pH 8.4 and 25 °C. $I = 0.10 \text{ M}$ (NaClO_4), $[\text{Ni}_2\text{L}] = 0.02 \text{ mM}$ and buffer solution (50 mM HEPPS). *Inset* Lineweaver–Burk double-reciprocal plot

8.4, the UV–vis spectrum of Ni_2L in buffer solution exhibited a strong absorption band at 505 nm, with the extinction coefficient of $90 \text{ M}^{-1}\text{cm}^{-1}$, assigned to the existence of square-planar four-coordinated Ni^{2+} in Ni_2L , as shown in an analogous asymmetric dinickel(II) system [18]. These results strongly suggest that $[\text{Ni}_2\text{L}(\text{OH})]^{2+}$ is the active species responsible for cleaving BNPP. Figure 3 shows the effect of Ni_2L concentrations on the value of k_{obs} for the cleavage of BNPP at pH 8.4 and 25 °C. The rate of BNPP cleavage initially increases linearly with increasing Ni_2L concentration, indicating the reaction is pseudo-first order for $[\text{Ni}_2\text{L}]$. The calculated pseudo-second-order rate constant for Ni_2L determined from the plot is $8.94 \times 10^{-3} \text{ M}^{-1} \text{ s}^{-1}$.

The initial rate of BNPP cleavage has also been determined as a function of the substrate concentration at pH 8.4. The data depicted in Fig. 4 reveal saturation kinetics with Michaelis–Menten-like behavior, typical for native metalloenzymes. The data points were fitted to the Michaelis–Menten model by means of a Lineweaver–Burk double-reciprocal plot, which resulted in a Michaelis constant (K_M) of $6.95 \times 10^{-3} \text{ M}$ and a catalytic rate constant ($k_{\text{cat}} = V_{\text{max}}/[\text{Ni}_2\text{L}]$) of $7.40 \times 10^{-5} \text{ s}^{-1}$. The second-order rate constant K_{BNPP} (k_{cat}/K_M) for BNPP is $1.06 \times 10^{-2} \text{ M}^{-1} \text{ s}^{-1}$. The reciprocal of the Michaelis–Menten constant could be treated as the substrate binding constant, that is, $K_b = 1/K_M = 143.9 \text{ M}^{-1}$. The low value of K_b is in agreement with the observations that BNPP is a weak ligand for Ni_2L [22, 23]. At pH 8.4 and 25 °C, the first-order rate constant ($k = k_{\text{OH}}[\text{OH}^-]$) for automatic hydrolysis of BNPP is calculated to be $1.46 \times 10^{-11} \text{ s}^{-1}$ with $k_{\text{OH}} = 5.8 \times 10^{-6} \text{ M}^{-1} \text{ s}^{-1}$ for BNPP ($V_{\text{auto}} = k_{\text{OH}}[\text{BNPP}][\text{OH}^-]$) [24]. Therefore, it can be concluded that at pH 8.4 and 25 °C, Ni_2L promotes the hydrolysis of BNPP by a factor of 5.1×10^6 . Under the same conditions,

Scheme 2 Proposed mechanism for hydrolysis of BNPP by Ni_2L



the catalytic activity of complex **1** was also measured, and it promoted the hydrolysis of BNPP by a factor of 7.8×10^4 , indicating that the bridging carboxyl group is an inhibitor of the catalytic species that reduces the rate of catalytic hydrolysis. This result further suggests that BNPP coordinates the two nickel centers by a bidentate bridging mode in the catalytic reaction.

Mechanism of catalytic phosphodiester hydrolysis

On the basis of the above studies, a double Lewis acid activation mechanism is proposed for the catalytic hydrolysis of BNPP by Ni_2L , which is similar to previously reported cases [18, 25, 26]. As shown in Scheme 2, the catalytic hydrolysis cycle may contain the following steps. First, the active species **A** is formed at pH 8.4, and then BNPP coordinates to the two nickel centers as a bidentate ligand, forming the BNPP adduct **B** (similar to the structure of **2**). Next, the bridging hydroxide acts as a nucleophile and attacks BNPP, forming a transition complex **C**. Third, the P–O bond in **D** breaks to release *p*-nitrophenolate followed by recovery of the starting complex **A**, accomplished by the replacement of NPP with hydroxide. In the first step, an equilibrium may exist between **A** and **B**, since BNPP is a weak ligand for Ni_2L . The intrinsic activity of a dinuclear catalyst is highly dependent upon the metal–metal distance [1]. The appropriate intermetallic separation (3.305 Å in complex **1** and 3.558 Å in **2**) can facilitate the phosphate bridging [26], and thus, BNPP is activated by the two nickel centers as in other dinuclear metallohydrolases [1,

22]. In addition, the two nickel centers bring together the two reactants (substrate BNPP and nucleophile OH^-), neutralizing the electrostatic repulsion that would occur for two negatively charged species.

Conclusions

In summary, we have developed a convenient and versatile procedure for the synthesis of a new asymmetric alkoxide-based dinucleating ligand. In the dinickel(II) complexes **1** and **2**, the ligand forces the two metal ions into proximity with different chemical environments, as in related natural dinuclear metalloenzymes. At 25 °C, the Ni_2L species formed in situ from a 2:1 mixture of Ni^{2+} and HL in aqueous solution at pH 8.4 shows efficient phosphodiesterase activity.

References

1. Parkin G (2004) Chem Rev 104:699
2. Mitić N, Smith SJ, Neves A, Guddat LW, Gahan LR, Schenk G (2006) Chem Rev 106:3338
3. Mancin F, Tecilla P (2007) New J Chem 31:800
4. Liu CL, Wang M, Zhang TL, Sun HZ (2004) Coord Chem Rev 248:147
5. Meyer F (2006) Eur J Inorg Chem 3789
6. Ren YW, Guo H, Wang C, Liu JJ, Jiao H, Li J, Zhang FX (2006) Transit Met Chem 31:611
7. Odonoghue A, Pyun SY, Yang MY, Morrow JR, Richard JP (2006) J Am Chem Soc 128:1615

8. Mancina F, Tecilla P (2007) *New J Chem* 31:800
9. Lu ZL, Liu T, Neverov AA, Brown RS (2007) *J Am Chem Soc* 129:11642
10. Subat M, Woinaroschy K, Gerstl C, Sarkar B, Kaim W, Knöig B (2008) *Inorg Chem* 47:4661
11. Mandal S, Balamurugan V, Lloret F, Mukherjee R (2009) *Inorg Chem* 48:7544
12. Arora H, Barman SK, Lloret F, Mukherjee R (2012) *Inorg Chem* 51:5539
13. Daumann LJ, Comba P, Larrabee JA, Schenk G, Stranger R, Cavigliasso G, Gahan LR (2013) *Inorg Chem* 52:2029
14. Fenton DE (2002) *Inorg Chem Commun* 5:537
15. Greatti A, Brito MA, Bortoluzzi AJ, Ceccato AS (2004) *J Mol Struct* 688:185
16. Greatti A, Scarpellini M, Peralta RA, Casellato A, Bortoluzzi AJ, Xavier FR, Jovito R, Brito MA, Szpoganicz B, Tomkowicz Z, Rams M, Haase W, Neves A (2008) *Inorg Chem* 47:1107
17. Ren YW, Wu AZ, Liu HY, Jiang HF (2010) *Transit Met Chem* 35:191
18. Ren YW, Lu JX, Cai BW, Shi DB, Jiang HF, Chen J, Zheng D, Liu B (2011) *Dalton Trans* 40:1372
19. Sheldrick GM (2008) *Acta Cryst A* A64:112
20. In respect to a pH-dependent equilibrium between *p*-nitrophenol (NP) and *p*-nitrophenolate (NPat), the increase of the concentration of the reaction product can be calculated ($\text{pH} = \text{p}K_a + \log [\text{NPat}]/[\text{NP}]$)
21. He C, Lippard SJ (2000) *J Am Chem Soc* 122:184
22. Vichard C, Kaden TA (2002) *Inorg Chim Acta* 337:173
23. Yatsimirsky AK (2005) *Coord Chem Rev* 249:1997
24. Humphry T, Forconi M, Williams NH, Hengge AC (2004) *J Am Chem Soc* 126:11864
25. Cox RS, Schenk G, Mitic N, Gahan LR, Hengge AC (2007) *J Am Chem Soc* 129:9550
26. Belle C, Gautier-Luneau I, Karmazin L, Pierre JL, Albedyhl S, Krebs B, Bonin M (2002) *Eur J Inorg Chem* 3087